Applied Catalysis A: General 415–416 (2012) 10–16

Contents lists available at SciVerse ScienceDirect

Applied Catalysis A: General

journal homepage: www.elsevier.com/locate/apcata

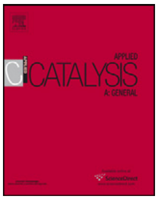

Oxidation of phenol to dihydroxybenzenes by nitrous oxide

D.P. Ivanov, L.V. Pirutko, G.I. Panov*

Boreskov Institute of Catalysis SB RAS, Novosibirsk 630090, Russia

ARTICLE INFO

Article history:
Received 20 October 2011
Received in revised form
24 November 2011
Accepted 25 November 2011
Available online 4 December 2011

Keywords:
Dihydroxybenzenes
Phenol oxidation
Phenol hydroxylation
N_2O
FeZSM-5
Hydroquinone
Resorcinol
Catechol

ABSTRACT

Gas phase oxidation of phenol by nitrous oxide for preparation of dihydroxybenzenes (DHB) is of significant interest. However, due to experimental difficulties caused by the high boiling points of DHB (240–285 °C), no detailed investigation of this reaction has been conducted until now. In the present work, the reaction was studied for the first time using a catalytic setup specially designed for operation with high-boiling compounds.

FeZSM-5 zeolites were shown to be efficient catalysts for the title reaction. An unusual isomeric distribution of DHB depending on reaction conditions was found. Formation of resorcinol, in addition to hydroquinone and catechol, is a particular feature of the reaction. Although the fraction of resorcinol averaged over 12 h time-on-stream is not high (6–9 mol.%), in the initial period of reaction it may comprise over 70% of the total amount of DHB.

A comparison with the current liquid-phase processes of phenol oxidation by H_2O_2 shows that the oxidation by N_2O may open a new promising way for alternative production of DHB in the gas phase.

1. Introduction

Dihydroxybenzenes (hydroquinone, resorcinol, and catechol) are important intermediates used in chemical, agrochemical, pharmaceutical and food industries. Present-day processes of their production are quite imperfect. Catechol (CH) and hydroquinone (HQ) are usually produced simultaneously by liquid phase oxidation (hydroxylation) of phenol with hydrogen peroxide. The strong acids $HClO_4$ and H_3PO_4 (Rhodia process), Fenton's reagent of Fe^{++}/Co^{++} (Brichima process) or TS-1 zeolite (Enichem process) are used as catalysts for this reaction [1]. In all cases, intense tar formation and H_2O_2 decomposition take place. The total dihydroxybenzenes (DHB) selectivity based on phenol is 80–90%, and that based on H_2O_2 is 50–70%.

The synthesis of resorcinol (RS) is usually conducted via an intermediate preparation of some aromatic *m*-isomers, viz. 1,3-benzenedisulfonic acid, which is then subjected to alkali fusion to form the desired product.

Currently, the oxidation of phenol to DHB is extensively studied in many laboratories to find more effective ways for implementation of this difficult reaction. Various metals, metal oxides, organic and inorganic metal complexes have been tested as catalysts using H_2O_2 oxidant in the liquid phase [2–7]. However, the progress seems to be rather modest.

The transfer of a reaction into the gas phase can provide some important technological advantages related, in particular, to continuous operation of the process, catalyst separation, and catalyst regeneration. In particular, the latter operation can be conveniently done in the same reactor by burning out carbonaceous deposits from the catalyst surface. Therefore, it would be of significant interest to develop a gas-phase process of phenol oxidation. Previous attempts to carry out this reaction in the gas phase using dioxygen proved unsuccessful because of the very low selectivity of DHB. One may expect that the use of nitrous oxide can give a more favorable prospect for this transformation:

$$C_6H_5OH + N_2O \rightarrow C_6H_4(OH)_2 + N_2 \tag{1}$$

Indeed, the related reaction of benzene oxidation to phenol by N_2O over FeZSM-5 zeolites proceeds with a very high selectivity [8–16]. The efficiency of these catalysts is due to the presence of α-sites, which are formed from admixed or specially introduced iron in the process of high-temperature zeolite activation [10,17–19]. The α-sites consist of reduced Fe^{II} complexes located in the micropore space of the zeolite matrix. A remarkable feature of α-sites is that they are inert to dioxygen, but are readily oxidized by nitrous oxide to generate a very reactive anion radical species of α-oxygen [8,11,17,20–22]:

$$N_2O + (Fe^{II})_\alpha \rightarrow (Fe^{III}\text{—}O^{-\bullet})_\alpha + N_2 \tag{2}$$

---

* Corresponding author.
E-mail address: panov@catalysis.ru (G.I. Panov).

0926-860X/$ – see front matter © 2011 Elsevier B.V. All rights reserved.
doi:10.1016/j.apcata.2011.11.029

Table 1
Characteristics of FeZSM-5 samples.

Samples	C_α (site/g)	Texture parameters			
		V_μ (cm^3/g)	V_Σ (cm^3/g)	A_{BET} (m^2/g)	A_{ext} (m^2/g)
1. Parent FeZSM-5 (500 °C, dry air)	0.5×10^{17}	0.165	0.275	443	75
2. Parent FeZSM-5 (steamed at 650 °C)	6.5×10^{17}	0.160	0.265	430	68
3. FeZSM-5/Al_2O_3 (500 °C, dry air)	0.5×10^{17}	0.100	0.390	390	155
4. FeZSM-5/Al_2O_3 (steamed at 650 °C)	2.7×10^{17}	0.085	0.400	345	144
5. FeZSM-5/Al_2O_3 (steamed at 750 °C)	1.7×10^{17}	0.080	0.350	335	138

A number of studies have shown that α-oxygen is involved in the hydroxylation of benzene. Especially convincing results were obtained by Uranov et al. [23] and Chernyavsky et al. [24], who showed that the rate of benzene oxidation increased linearly by about 2 orders of magnitude with increasing the concentration of α-sites.

As for the oxidation of phenol, this reaction has not previously been studied in detail. It was first mentioned in [25] with reference to patent [26]. The patent is mainly focused on the oxidation of benzene, suggesting also some examples with other aromatic compounds, including phenol. Costine et al. [27] tested phenol in line with some other aromatic molecules to elucidate the effect of a substituent nature on their reactivity toward N_2O. In both cases, the oxidation of phenol provided DHB products comprising only HQ and CH with a total selectivity of 92–98%. The latter values are certainly overestimated since the selectivities were calculated without taking coke into account, which, as we will see below, may have a significant effect on the results. Ivanov et al. [28] investigated the oxidation of phenol in its mixture with benzene. The authors showed that benzene significantly improved stability and selectivity of the reaction. However, they could use only minor concentrations of phenol in the feed (4.6%) to prevent plugging of the setup gas lines by condensing DHB products. Therefore, productivity of the reaction was very low.

The lack of detailed studies on phenol oxidation by N_2O is due to significant experimental difficulties caused by the high boiling points of DHB. In conventional catalytic setups, the temperature of the gas lines usually does not exceed 180 °C. Since the boiling points of CH, RS, and HQ are 240, 281 and 285 °C, respectively, this temperature is not high enough to prevent their condensation. It leads to an increasing resistance to the feed flow with time-on-stream, and ultimately to the failure of the run. This problem is discussed in [28].

In the present work, the oxidation of phenol by N_2O was studied for the first time using a catalytic setup specially designed for operation with high-boiling compounds. The temperature of the analytical part of the setup can be maintained at up to 330 °C. The obtained results revealed high catalytic potential of FeZSM-5 zeolites, which open a new promising way for preparation of DHB.

2. Experimental

2.1. Catalysts

A parent FeZSM-5 zeolite was prepared according to [29]. Its chemical composition in H-form comprises 0.9 wt.% Al, 0.01 wt.% Na, and 0.03 wt.% Fe (ICP data). This composition was specially designed to provide a small Fe concentration, which would allow one to conduct reaction at a rather high temperature thus ensuring an efficient desorption of DHB from the catalyst surface. Under this condition, an excess concentration of iron and consequently that of α-sites may lead to overoxidation of the products. Texture parameters of the zeolite (micropore volume, V_μ; total pore volume, V_Σ; BET surface area, A_{BET}; and external surface area, A_{ext}) obtained with the low-temperature N_2 adsorption are typical of the MFI structure (Table 1). High crystallinity of the zeolite as well as the absence of foreign phases are evidenced by XRD data collected both before and after its activation (Fig. SM. 1 in supplementary material section).

The parent FeZSM-5 zeolite (sample 1, Table 1) was used for preparation of formed catalysts. For that, the zeolite was mixed with boehmite peptized by dilute HNO_3 (65 wt.% FeZSM-5 and 35 wt.% of the boehmite). Afterwards, the material was extruded using a die of 3 mm diameter, dried at 383 K and calcined in dry air at 773 K (sample 3, Table 1). A calculated composition of the formed and calcined catalyst corresponds to 70 wt. % of the zeolite and 30 wt.% of Al_2O_3 binder. Activation of the catalyst was done by steaming in a He flow containing 50 mol.% H_2O at two different temperatures: one sample at 650 °C and the other one at 750 °C (samples 4 and 5 in Table 1). Further in the text, the activated samples will be referred to as FeZSM-5 (650 °C), FeZSM-5/Al_2O_3 (650 °C) and FeZSM-5/Al_2O_3 (750 °C), accordingly.

From texture parameters presented in Table 1 one can see that both the forming procedure and the steam activation of the formed samples lead to a decrease of V_μ. In the case of formed catalysts, it probably resulted from a partial sealing of micropores by a binder. Since α-sites locate precisely in the micropore space [8,13,30–32], it resulted in a drop of the α-site concentration (C_α): from 6.5×10^{17} site/g for the parent zeolite to 2.7×10^{17} and 1.7×10^{17} site/g for the formed samples (Table 1).

The value of C_α was calculated from the N_2 amount evolved at the N_2O decomposition at 230 °C. At this temperature the reaction proceeds stoichiometrically according to Eq. (2). Additionally, the isotopic exchange of α-oxygen $^{16}O_\alpha$ with dioxygen $^{18}O_2$ was conducted at 100 °C, providing similar results. In more detail, procedures for measuring the concentration of α-sites are given elsewhere [31,33].

2.2. Flow setup

Catalytic experiments were performed in an automated flow setup having a high-temperature switching valves with rotors made of "polyamide/PTFE/carbon" composite, which operating temperature is 150–330 °C (Valco Instrument Co., Inc.). Analytical part of the setup was accommodated in a ventilated thermal box at 290 °C. This temperature prevents condensation of the reaction products and provides a reliable on-line GC analysis. A picture of the setup and a typical on-line chromatographic pattern are presented in Figs. SM. 2 and SM. 3 of the supplementary material section.

To conduct catalytic runs, 1 g of a catalyst (0.5–1.0 mm particles) was placed into a quartz reactor with the inner diameter 7 mm. Before testing, the catalyst was treated in flowing air at 550 °C. Nitrous oxide and helium were fed by flow mass controllers (MKS Instruments); phenol of C.P. grade was fed by a high-performance syringe pump 500 D (ISCO) capable of keeping phenol in a liquid state at 60 °C.

The reaction mixture was automatically sampled and analyzed each 16 min. Analysis of N_2O and N_2 was performed at room temperature using a packed column filled with Porapak Q and TCD. For a more accurate CO_x measurement, carbon oxides were first

Table 2
Data on the oxidation of phenol by N_2O averaged over 12 h runs.

Run no.	Reaction conditions			DHB productivity (mmol/(g h))	Conversion (%)		Selectivities based on PhOH (%)				$S_{DHB(N_2O)}$ (%)	DHB distribution (%)					Coke; Deactivation	
	T (°C)	N_2O:PhOH (mol.%)	t_{res} (s)		PhOH	N_2O	DHB	CO_x	Side products	Coke		HQ	CH	RS	BQ	HQ + BQ	m_{coke} (g/g_{cat})	D (%)
1	475	3:30	1.7	1.7	4.2	43	83	4.2	2.0	10.8	76	48	37	6	9	57	0.24	20
2	450	3:30	1.7	0.85	2.3	22	79	3.0	3.5	14.4	83	45	37	7	11	56	0.18	~5
3	500	3:30	1.7	1.9	5.1	70	82	5.5	2.5	10.0	60	52	36	7	5	57	0.28	35
4	475	1.5:30	1.7	0.85	2.2	48	80	4.2	3.6	11.8	83	53	33	9	5	58	0.14	~5
5	475	5:30	1.7	2.3	5.9	40	86	3.8	1.7	8.4	74	46	39	6	9	55	0.32	45
6	475	3:30	3.4	1.1	5.0	69	80	3.7	2.3	14.0	65	60	30	8	2	62	0.19	10
7	475	3:30	1.7	1.6	4.1	45	82	4.3	2.1	10.6	72	48	38	6	8	56	0.22	20

hydrogenated over a nickel catalyst and then analyzed as methane using FID. Analysis of organic compounds was performed at a programmed temperature elevation from 180 to 280 °C with a capillary column DB-1701 (J&W Scientific) using FID. In run no. 1 (Table 2), the reaction products were accumulated and analyzed by GC–MS method, which results well agree with the results of on-line GC analysis.

Chromatographic data were used to calculate main parameters of the reaction presented in Table 2: DHB productivity (Pr); conversions of phenol and N_2O (X_{PhOH}, X_{N_2O}); selectivities of their transformation to DHB, CO_x and side products; isomeric distribution of DHB; and catalyst deactivation. Equations used for calculation of the aforementioned parameters are presented in supplementary material section.

The carbon material balance was very close to 100%, which is theoretically expected at low phenol conversions used in the work (2.2–5.9%). The oxygen material balance defined as the sum of oxygen containing products vs. the N_2O conversion was 100 ± 5%. In the very initial period of reaction the balance may drop down to 85%.

2.3. Regeneration and coke amount

In the reaction course, the catalyst deactivates due to coke formation. After the reaction completion, coke was carefully burned out to determine its amount (m_{coke}) and regenerate the catalyst. For that, the sample was first blown off at 500 °C in flowing helium for 30 min. Carbonic deposits, not removed from the surface under these conditions, were considered as coke. The burning out was performed in flowing helium with 10 mol.% air, at a gradual temperature elevation from 450 to 550 °C. The value of m_{coke} expressed in gram of coke per gram of catalyst (g/g_{cat}) was calculated from the total amount of CO_x assuming coke elementary composition to be identical to that of phenol. Some control TGA measurements provided well-consistent results on the coke amount. The coke burning out resulted in complete restoration of the initial catalytic activity.

3. Results

3.1. Catalyst selection for detailed study

First, we performed preliminary catalytic experiments for selecting a suitable sample for the further detailed study. For that, all three activated samples (nos. 2, 4, 5 of Table 1) were tested under identical conditions: 475 °C, residence time 1.7 s, mole ratio N_2O:PhOH = 3:30, He balance. Results are shown in Fig. 1 as a total DHB productivity vs. time-on-stream. One can see that in all cases, a significant increase of productivity takes place in the initial period. Such phenomenon is known to occur sometimes as a result of catalyst activation (working up) due to a tuning of the surface chemical composition by reaction mixture [34]. But this is obviously not the case with FeZSM-5 catalysts. Numerous data on the oxidation of benzene to phenol by N_2O showed that in the initial period the catalyst has the highest activity, which gradually decreases with time-on-stream due to coking. In our case, regarding high boiling points of DHB, one may think that the low initial activity is most likely related to intense adsorption of the reaction products. Upon completion of the adsorption, the activity achieves its maximum value and then gradually decreases due to continuing coking process.

Fig. 1 clearly reveals different activity of the samples, which can be inferred from their maximum productivity. The parent FeZSM-5 zeolite providing 2.7 mmol/(g h) is the most active sample. The formed samples have lower productivities: 1.9 mmol/(g h) and 1.2 mmol/(g h) depending on the activation temperature. This activity sequence correlates with the concentration of α-sites, which decreases in the same order, from 6.5×10^{17} to 2.7×10^{17} and 1.7×10^{17} site/g, respectively.

Another important result seen in Fig. 1 is a beneficial effect of Al_2O_3 binder on the catalytic stability. This is evidenced by a much slower deactivation of both formed samples with the time-on-stream. Based on a favorable combination of activity and stability, we selected the FeZSM-5/Al_2O_3 (650 °C) catalyst for a more detailed study. All further data were collected with this sample.

3.2. Results of run no. 1

Oxidation of phenol over the FeZSM-5/Al_2O_3 (650 °C) sample was studied at different temperatures, feed mixture composition, and residence time. Results are collected in Table 2. For a better understanding of the parameters under consideration, we will comment below upon Fig. 2 presenting results of the run no. 1.

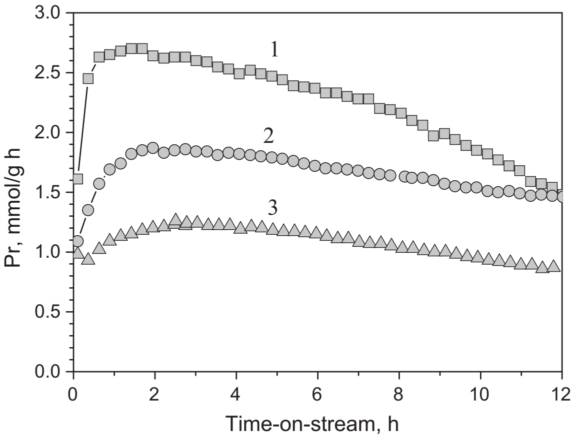

Fig. 1. DHB productivity vs. time-on-stream: (1) FeZSM-5 (650 °C); (2) FeZSM-5/Al_2O_3 (650 °C); (3) FeZSM-5/Al_2O_3 (750 °C). Reaction conditions: 475 °C; N_2O:PhOH = 3:30 mol.%; residence time 1.7 s.

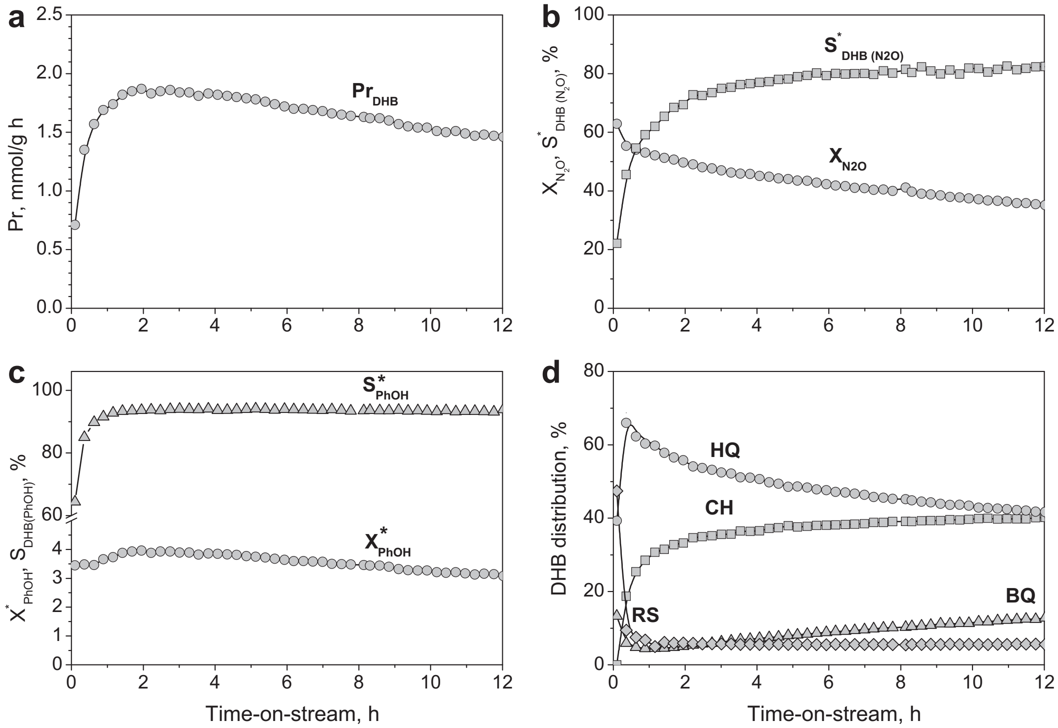

Fig. 2. Variation of reaction parameters with time-on-stream in run no. 1 (for reaction conditions see Table 2): (a) DHB productivity; (b) N_2O conversion (X_{N_2O}) and DHB selectivity based on N_2O, $S_{DHB(N_2O)}$; (c) phenol conversion (X^*_{PhOH}) and DHB selectivity based on phenol, $S^*_{DHB(PhOH)}$; and (d) isomeric distribution of DHB.

Fig. 2a shows how the catalyst productivity varies with time-on-stream, which shortly has been outlined above. In the initial period, Pr significantly increases starting from 1.1 mmol/(g h) and achieving in 2 h 1.9 mmol/(g h). Then, nearly a linear decrease of Pr is observed, which becomes 1.5 mmol/(g h) at 12 h time-on-stream. It means that to the end of run the catalyst retains 80% of its maximum activity. The productivity averaged over the 12 h operation is 1.7 mmol/(g h).

Fig. 2b shows reaction parameters related to N_2O. The DHB selectivity based on nitrous oxide ($S_{DHB(N_2O)}$) grows substantially: from 22% at the beginning of the run to 82% at its end. Meanwhile, N_2O conversion (X_{N_2O}) shows an opposite trend, monotonically decreasing from 62% to 35%.

Fig. 2c illustrates similar parameters related to phenol. In this case, the symbols of phenol conversion (X^*_{PhOH}) and DHB selectivity based on phenol ($S^*_{DHB(PHOH)}$) are marked by an asterisk to indicate that these parameters are calculated without regard for coke (values of m_{coke} were measured upon termination of the runs). In the initial period of reaction, the value of $S^*_{DHB(PHOH)}$ rises from 64% to 94% and then remains virtually constant. The value of X^*_{PhOH} changes only slightly, having a weak maximum at 2 h. However, this maximum is likely a seeming event resulting from the method of X^*_{PhOH} calculation, based on the amount of products recorded. As noted above, at the initial time the products are intensely consumed for adsorption and coking, thus giving underrated initial values of X^*_{PhOH}.

Unusual changes are observed with the isomeric distribution of DHB. Fig. 2d presents fractions of HQ, CH, RS and BQ (*p*-benzoquinone; the latter compound we also consider as DHB). One can see that all the isomers behave differently. Most strong changes occur at the very beginning of the reaction. Thus, with the reaction time increasing from 6 min (first point) to 22 min (second point), HQ fraction increases from 39% to 67%, RS fraction decreases from 47% to 10%, CH fraction increases from zero to 19%, and BQ fraction decreases from 13% to 6%. After that, HQ gradually decreases to 42%, CH rises to 40%, while RS goes to a stationary value of ca. 6%. BQ, which may result from oxidation of HQ, passes a minimum and then linearly increases to 13%.

Upon averaging over 12 h, run no. 1 provides the following results (Table 2): DHB productivity is 1.7 mmol/(g h); phenol conversion is 4.2%; and N_2O conversion is 43%. DHB selectivity based on phenol is 83%. The rest 17% of phenol transforms into CO_x (4.2%); the sum of side organic products, mainly dibenzofuran and phenoxyphenols (2.0%); and coke (10.8%). DHB selectivity based on N_2O is 76%. Fractions of DHB isomers are as follows: 48% HQ, 37% CH, 6% RS, and 9% BQ. The total fraction of *p*-isomers (HQ + BQ) comprises 57%. The mass of coke accumulated on the catalyst charge (1 g) is 0.24 g; the catalyst deactivation is 20%.

Run no. 7 was conducted under the same conditions as run no. 1 to verify the reproducibility of results, which proved to be satisfactory.

3.3. *Effect of reaction conditions*

This effect will be discussed using mainly the averaged data of Table 2. These data were calculated taking into account (where appropriate) the amount of coke, m_{coke}, formed on the catalyst during the run.

3.3.1. *Temperature*

From Table 2 one can see that raising the reaction temperature from 450 to 500 °C (runs 1–3) increases the DHB productivity from 0.85 to 1.9 mmol/(g h). A pronounced increase is observed also for conversion of both phenol (2.3% → 5.1%) and nitrous oxide (22 → 70%). Interestingly, DHB selectivity based on phenol shows only a minor change (79–83%), whereas that based on N_2O drops substantially: from 83% at 450 °C to 60% at 500 °C. This drop is accompanied by an increase in selectivity to CO_x (3.0 → 5.5%), which formation may proceed mainly due to oxidation of coke.

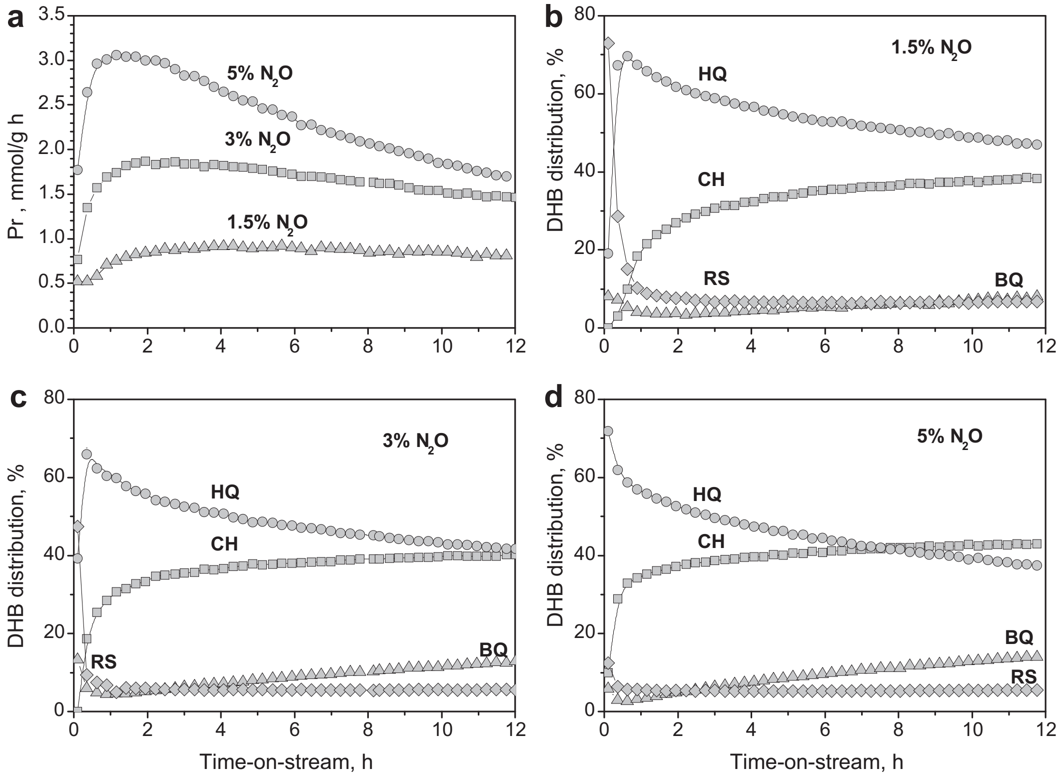

Fig. 3. Effect of N_2O concentration on DHB productivity (a) and DHB distribution (b, c, d). For reaction conditions see Table 2, runs 1, 4, 5.

Indeed, as selectivity to CO_x increases, the selectivity to coke decreases (14.5% → 10%).

The DHB distribution proved to be low sensitive to the temperature. Fractions of CH (36–37%) and RS (6–7%) remain virtually constant. An increase in HQ fraction (45 → 52%) with temperature elevation is compensated by a decreasing fraction of BQ (11 → 5%). So, the sum of *p*-isomers also remains nearly constant (56–57%).

Temperature elevation strongly increases the catalyst deactivation. Thus, at 450 °C deactivation is weak, ~5%, whereas at 500 °C it is 35%.

3.3.2. Feed composition

Fig. 3a illustrates changes in the catalyst productivity with the time-on-stream at different concentrations of nitrous oxide (C_{N_2O}) in the feed mixture: 1.5% N_2O, 3.0% N_2O and 5.0% N_2O. In all cases, phenol concentration is 30 mol.%, and temperature is 475 °C. It is seen that the growth of C_{N_2O} increases both productivity and deactivation of the catalyst. Indeed, Table 2 (runs 1, 4, 5) indicates that the averaged productivity at 1.5% N_2O is 0.85 mmol/(g h), whereas at 5% N_2O it is 2.3 mmol/(g h). Simultaneously, the deactivation rises from ~5% to 45%. The increase in C_{N_2O} is accompanied by a considerable growth of phenol conversion (2.2% → 5.9%) and some decrease of N_2O conversion (48 → 40%). At the same time, phenol selectivity to DHB rises (80 → 86%), while N_2O selectivity falls (83 → 74%).

Fig. 3b–d shows changes in the isomeric distribution of DHB. In all cases, HQ and CH are predominant products, their fractions differently depending on both the N_2O concentration and especially the time-on-stream. Thus, with $C_{N_2O} = 1.5\%$, the ratio HQ:CH at 1 h of time-on-stream is 3.3, whereas at 12 h it is 1.2. Variations in the averaged distribution (Table 2) are not so significant. The most noticeable change is for HQ, which fraction decreases from 53% to 46% as C_{N_2O} increases. However, the total *p*-isomer fraction (HQ + BQ) varies only slightly, 55–58%.

3.3.3. Residence time

Runs no. 1 and no. 6 (Table 2) were conducted under similar conditions, except for the residence time (t_{res}), which was 1.7–3.4 s, respectively. An increase of t_{res} raises the conversion of both phenol and nitrous oxide, but decreases the productivity (1.7 → 1.1 mmol/(g h)). Other essential changes are as follows: a decrease of N_2O selectivity to DHB (76 → 65%); an increase of phenol selectivity to coke (10.8 → 14.0%); and an increase of HQ fraction (48 → 60%). Changes of the total *p*-isomer fraction are less significant (57 → 62%).

4. Discussion

4.1. Catalyst deactivation

In the liquid phase oxidation by hydrogen peroxide, 10–20% of phenol is consumed for tar formation [1]. In our case, coke is formed instead of tar, being responsible for 8.4–14.4% of the phenol consumed (Table 2). There is a correlation between coke amount and catalyst deactivation. Indeed, run no. 5 with $m_{coke} = 0.32\ g/g_{cat}$ shows the highest deactivation (45%), whereas runs no. 2 and no. 4 with m_{coke} of 0.18 and 0.14 g/g_{cat} show the least one (~5%). However, amount of coke does not correlate with the phenol selectivity to coke, since m_{coke} depends also on the reaction rate. With increase of the rate, the amount of coke increases, but not so strongly as the DHB productivity. Therefore, run no. 5 with the largest value of m_{coke} has the lowest phenol selectivity to coke, 8.4%.

It is generally accepted that coke formation on zeolite surfaces is mediated by both the Bronsted and the Lewis acid sites. But the mechanism of its deactivating effect is less clear. It may relate to both the diffusion limitations and the poisoning of active sites. The mechanism of FeZSM-5 deactivation in the oxidation of benzene to phenol by N_2O was thoroughly studied in [30,35]. A loss in activity was shown to result from coke deposition in the zeolite micropores, which is exactly the place of α-sites location [8,13,32]. Coke decreases the number of operating sites, but the turnover frequency calculated per a single operating site remains constant irrespective of the coke amount and deactivation degree. This result clearly testifies that deactivation is caused by poisoning of active sites rather than by difficult diffusion of the reactants to and from the sites.

Most likely, this deactivation mechanism holds also for the oxidation of phenol to DHB. But taking into account a much more intense coking in the latter reaction, one can assume that deactivation in this case may be additionally aggravated also by worsening of the reactants diffusion or partial blocking of micropores due to coking of the external surface of zeolite. In particular, this assumption may explain an improved stability of the formed samples compared to that of the parent zeolite. Due to Al_2O_3 binder, the formed samples have a much greater external surface area (Table 1), which may be a suitable depot for accumulation of external coke not decreasing the catalytic activity.

4.2. Isomeric distribution of DHB

As we could see above, the oxidation of phenol by N_2O leads to all three DHB isomers, which is not typical of the oxidation by H_2O_2. In the aromatic ring, the OH group is known to activate the *o*- and *p*-positions, but deactivate the *m*-position. This phenomenon explains why only CH and HQ form at phenol oxidation by H_2O_2 [2–7]. In this case, the OH radicals (e.g. in Fenton system) or the peroxide groups bound to isolated metal atoms (e.g. on TS-1) are supposed to be active oxidants [36], which reactivity is not enough to attack the *m*-position. In the case of N_2O, the active oxidant is α-oxygen, which is a radical species $O^{\bullet -}$ bound to iron. Because of a very high reactivity of α-oxygen [8,37,38], the difference between activated and non-activated positions of phenol may become less important, leading to hydroxylation of *m*-position, too.

As noted above, the isomeric distribution of DHB strongly varies with the time-on-stream. According to a generally accepted idea, this variation can be explained by a transport limitation in the catalyst pore system imposed by coke. This limitation may change the composition of reaction products in favor of the molecules having smaller cross-sections and therefore greater diffusivities. However, this explanation, being verified in many cases, has a difficulty with our results. According to the above reasoning, one may expect that with increasing reaction time the fractions of CH and RS should decrease, while the fraction of HQ (its molecules have the smallest cross-section) should increase. But the actual changes are quite different. In Fig. 3b and c, neglecting the very initial time, one can see that HQ fraction monotonically decreases, whereas CH fraction increases and RS fraction remains nearly constant. So, some other ideas are needed for explaining this phenomenon. In particular, one should possibly take into consideration stability of DHB products under the reaction conditions, as well as their possible isomeric redistribution, which may take place on the external surface covered by coke. This important point is worth a further study.

Note that in the case of phenol oxidation by hydrogen peroxide no significant variation of DHB distribution with the reaction time was observed [3].

It is interesting to consider the DHB distribution at a minimum amount of coke on the surface, i.e. at the very initial reaction time (6 min). The initial isomeric fractions obtained at 475 °C with different N_2O concentrations (first points in Fig. 3b–d) are shown in Fig. 4. As C_{N_2O} rises from 1.5% to 5%, the fraction of RS strongly decreases (73 → 12%) and the fraction of HQ increases (18 → 72%), nearly compensating each other. Amounts of CH and BQ are rather insignificant and do not affect much a general picture. Remarkably, when dependences in Fig. 4 are extrapolated to $C_{N_2O} = 0$, the fraction of RS tends to 100%, whereas all other fractions tend to zero.

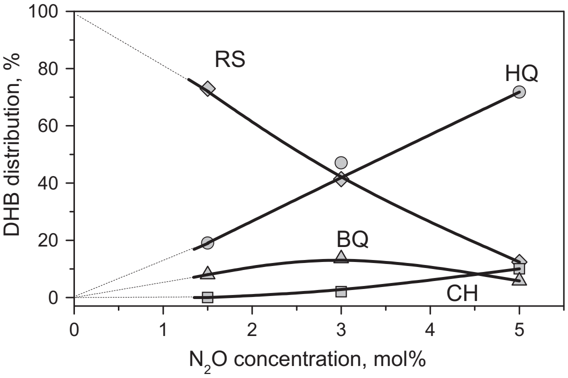

Fig. 4. Effect of N_2O concentration in the feed on the initial DHB distribution (Table 2, runs 1, 4, 5).

One can hardly think that this picture gives a real reaction pattern on a "clean" (non-coked) catalyst surface. Quite probably, this behavior is a result of an interplay of several factors like a different involvement of isomeric molecules in the adsorption, coke formation, and other processes, which proceed most intensely in the initial period. Identification of parameters affecting the distribution of DHB would be of significant interest.

4.3. Comparison with the present-day processes

The formed FeZSM-5/Al_2O_3 (650 °C) catalyst studied in this work is certainly not optimal. Its performance can be improved by tuning the chemical composition, preparation procedure, activation conditions, etc. Nevertheless, it seems interesting to compare the obtained results with the present-day processes of phenol oxidation to DHB. It may allow one to estimate whether these laboratory data can serve as a potential bases for developing a new DHB process, or they are too inferior for having such a prospect. The comparison can be made using the data of Table 3, composed by Notari [1] for the liquid-phase phenol oxidations with H_2O_2. Corresponding parameters for the N_2O oxidation are added from our Table 2, run no. 5.

One can see that in the case of N_2O, phenol conversion (5.9%) is on a level with Rhone Poulenc process (5%), but ranks below Brichima (10%) and particularly Enichem (25%) processes.

Phenol selectivity to DHB in the case of N_2O (86%) takes an intermediate position: it is somewhat lower than the selectivity of Rhone Poulenc and Enichem processes (both 90%) and higher as compared to Brichima (80%).

With both oxidants, a considerable fraction of phenol transforms into coke or tar. With N_2O, the proper phenol selectivity to coke is 8.4%. However, to provide a fair comparison with the selectivity to tar in the case of H_2O_2, this value should be added with the selectivities to CO_x and side products, which are virtually absent in the case of liquid-phase processes. Being summed up, they give 14%, which is somewhat higher than phenol selectivity to tar for Enichem (12%), but lower than that for Brichima (20%).

Nitrous oxide selectivity to DHB (74%) exceeds the selectivities of all H_2O_2 based processes (50–70%).

Since HQ is a more valuable product than CH, the ratio HQ:CH is considered to be an important parameter [1]. In the case of nitrous oxide, the HQ:CH ratio is equal to 1.2 (or 1.4 if BQ is taken into account). With this parameter, N_2O surpasses the H_2O_2 based processes, including the process on TS-1, where this ratio has the highest value equal to 1.0.

Summarizing the above comparison, we should admit that a formal ranging of processes are quite questionable. Efficiency of a process is determined by several parameters, sometimes

Table 3
Comparison of DHB preparation via phenol oxidation by N_2O and H_2O_2.

Process parameters	Oxidation by N_2O (run no. 5, Table 2)	Oxidation by H_2O_2 [1]		
		Rhone Poulenc ($HClO_4$, H_3PO_4)	Brichima (Fe^{++}/Co^{++})	Enichem (TS-1)
Phenol conversion, %	5.9	5	10	25
Phenol selectivity to DHB, %	86	90	80	90
Phenol selectivity to coke or tars, %	8.4 (14.0[a])	10	20	12
N_2O (H_2O_2) selectivity to DHB, %	74	70	50	70
HQ:CH ratio	1.2 (1.4[b])	0.71	0.43	1.0

[a] CO_x and side products are included in coke.
[b] The ratio calculated for the sum of (HQ + BQ).

differently directed. Nevertheless, one can see that parameters provided by N_2O are comparable with those provided by H_2O_2. It may open a new way for alternative preparation of DHB. In this connection, it is appropriate to note that nitrous oxide is not considered anymore as an exotic "laughing gas" as it was the case two decades ago. Nowadays it is a rather conventional compound whose unique oxidation chemistry is well studied, and appreciated not only in laboratory research but also in industry [8,31,39]. Recently, two new commercial oxidation processes have been put in operation first using the N_2O oxidant [40].

5. Conclusion

A formed FeZSM-5 zeolite, having small concentration of iron and accordingly that of α-sites, was studied in detail at 450–500 °C in the oxidation of phenol to DHB by nitrous oxide. For the first time the reaction was carried out in an automated catalytic setup specially designed for the gas-phase operation with high-boiling compounds. It allowed safe catalytic runs with reliable on-line GC analysis. The results obtained were completed with the data on coke amount. Deposition of coke on the catalyst surface was shown to cause a pronounced variation in the isomeric distribution of DHB, which does not correlate with diffusivities of the product molecules.

A comparison with the present-day processes based on H_2O_2 application shows that phenol oxidation by N_2O may be considered as a promising basis for developing an alternative technology of DHB preparation.

Supplementary material

The manuscript has a supplementary material section. It includes: XRD patterns of parent FeZSM-5 zeolite before and after activation; a picture of catalytic setup used in the work; a typical pattern of on-line GC analysis; and a list of equations used for calculating main reaction parameters.

Acknowledgements

This work was supported by RFBR (Grant No. 11-03-00427-a). The authors are grateful to E.V. Starokon for the measurement of α-sites concentration, and to A.S. Kharitonov for valuable comments.

Appendix A. Supplementary data

Supplementary data associated with this article can be found, in the online version, at doi:10.1016/j.apcata.2011.11.029.

References

[1] B. Notari, Stud. Surf. Sci. Catal. 37 (1988) 413–425.
[2] J. Sun, X. Meng, Y. Shi, R. Wang, S. Feng, D. Jiang, R. Xu, F.-S. Xiao, J. Catal. 193 (2000) 199–206.
[3] S. Seelan, A.K. Sinha, Appl. Catal. A: Gen. 238 (2003) 201–209.
[4] K. Yube, M. Faruta, N. Aoki, K. Mal, Appl. Catal. A: Gen. 327 (2007) 278–286.
[5] K.M. Parida, S. Singha, P.C. Sahoo, Catal. Lett. 136 (2010) 155–163.
[6] H.S. Abbo, S.J.J. Titinchi, Top. Catal. 53 (2010) 254–264.
[7] E.A. Karakhanov, A.L. Maximov, Y.S. Kardasheva, V.A. Skorkin, S.V. Kardashev, V.V. Predeina, M.Y. Talanova, E. Lurie-Luke, J.A. Seeley, S.L. Cron, Appl. Catal. A: Gen. 385 (2010) 62–72.
[8] G.I. Panov, CATTECH 4 (2000) 18.
[9] J. Jia, K.S. Pillay, W.M.H. Sachtler, J. Catal. 221 (2004) 119–126.
[10] I. Yuranov, D.A. Bulushev, A. Renken, L. Kiwi-Minsker, Appl. Catal. A: Gen. 319 (2007) 128–136.
[11] L.V. Pirutko, S.V. Chernyavsky, A.K. Uriarte, G.I. Panov, Appl. Catal. A: Gen. 227 (2002) 143–157.
[12] E.J.M. Hensen, Q. Zhu, M.M.R.M. Hendrich, A.R. Overweg, P.J. Kooyman, M.V. Sychev, R.A. van Santen, J. Catal. 221 (2004) 560–574.
[13] A. Ribera, I.W.C.E. Arends, S. de Vries, J. Perez-Ramires, R.A. Sheldon, J. Catal. 195 (2000) 287–297.
[14] G. Centi, S. Perathoner, R. Arrigo, G. Giordano, A. Katovic, V. Pedula, Appl. Catal. A: Gen. 307 (2006) 30–41.
[15] A.J.J. Koekkoek, H. Xin, Q. Yang, C. Li, E.J.M. Hensen, Micropor. Mesopor. Mater. 145 (2011) 172–181.
[16] D. Meloni, R. Monac, V. Solianas, G. Berlier, S. Bordiga, I. Rossetti, C. Oliva, L. Forni, J. Catal. 214 (2003) 169–178.
[17] K.A. Dubkov, N.S. Ovanesyan, A.A. Shteinman, E.V. Starokon, G.I. Panov, J. Catal. 207 (2002) 341–352.
[18] L. Kiwi-Minsker, D.A. Bulushev, A. Renken, J. Catal. 219 (2003) 273–285.
[19] A.R. Overweg, M.W.J. Craje, A.M. van der Kraan, J.W.C.E. Arends, A. Ribera, R.A. Sheldon, J. Catal. 223 (2004) 262–270.
[20] G.D. Pirngruber, J.-D. Grunwaldt, P.K. Roy, J.A. van Bokhoven, O. Safonova, P. Glatzel, Catal. Today 126 (2007) 127–134.
[21] E. Berrier, O. Ovsitser, E.V. Kondratenko, M. Schwidder, W. Grünert, A. Brückner, J. Catal. 249 (2007) 67–78.
[22] J.B. Taboada, E.J.M. Hensen, I.W.C.E. Arends, G. Mul, A.R. Overweg, Catal. Today 110 (2005) 221–227.
[23] I. Yuranov, D.A. Bulushev, A. Renken, L. Kiwi-Minsker, J. Catal. 227 (2004) 138–147.
[24] V.S. Chernyavsky, L.V. Pirutko, A.K. Uriarte, A.S. Kharitonov, G.I. Panov, J. Catal. 245 (2007) 466–469.
[25] G.I. Panov, A.S. Kharitonov, V.I. Sobolev, Appl. Catal. A: Gen. 98 (1993) 1–20.
[26] US Patent 5110995 (1992).
[27] A. Costine, T. O'Sillivan, B.K. Hodnett, Catal. Today 99 (2005) 199–208.
[28] D.P. Ivanov, V.I. Sobolev, L.V. Pirutko, G.I. Panov, Adv. Synth. Catal. 344 (2002) 986–995.
[29] E.G. Derouane, S. Determmerie, Z. Gabelica, N. Blom, Appl. Catal. 1 (1981) 201–224.
[30] D.P. Ivanov, M.A. Rodkin, K.A. Dubkov, A.S. Kharitonov, G.I. Panov, Kinet. Catal. 41 (2000) 771–775.
[31] G.I. Panov, A.K. Uriarte, M.A. Rodkin, V.I. Sobolev, Catal. Today 41 (1998) 365–385.
[32] L.V. Pirutko, O.O. Parenago, E.V. Lunina, A.S. Kharitonov, L.G. Okkel, G.I. Panov, React. Kinet. Catal. Lett. 52 (1994) 275–283.
[33] M.V. Parfenov, E.V. Starokon, S.V. Semikolenov, G.I. Panov, J. Catal. 263 (2009) 173–180.
[34] G.K. Boreskov, Heterogeneous Catalysis, Nova Sci. Publ. Inc., NY, 2002, 236 p.
[35] D.P. Ivanov, V.I. Sobolev, G.I. Panov, Appl. Catal. A: Gen. 241 (2003) 113–121.
[36] C. Perego, A. Carati, P. Ingallina, M.A. Mantegazza, G. Belussi, Appl. Catal. A: Gen. 221 (2001) 63–72.
[37] K.A. Dubkov, V.I. Sobolev, E.A. Talsi, M.A. Rodkin, N.H. Watkins, A.A. Shteinman, G.I. Panov, J. Mol. Catal. 123 (1997) 155–161.
[38] G.I. Panov, K.A. Dubkov, E.V. Starokon, Catal. Today 117 (2006) 148–155.
[39] V.N. Parmon, G.I. Panov, A. Uriarte, A.S. Noskov, Catal. Today 100 (2005) 115–131.
[40] BASF News Release, http://www.chemicalonline.com/article.mvc/BASF-Starts-Up-A-New-Production-Facility-For-0001, November 30, 2009.